SANDIA REPORT

SAND2014-2858
Unlimited Release
Printed April 2014
Supersedes SAND2012-5961 dated July 2012

A Simple Model of Gas Flow in a Porous Powder Compact

Andrew D. Shugard and David B. Robinson

Prepared by
Sandia National Laboratories
Albuquerque, New Mexico 87185 and Livermore, California 94550

Sandia National Laboratories is a multi-program laboratory managed and operated by Sandia Corporation, a wholly owned subsidiary of Lockheed Martin Corporation, for the U.S. Department of Energy's National Nuclear Security Administration under contract DE-AC04-94AL85000.

Approved for public release; further dissemination unlimited.

Issued by Sandia National Laboratories, operated for the United States Department of Energy by Sandia Corporation.

NOTICE: This report was prepared as an account of work sponsored by an agency of the United States Government. Neither the United States Government, nor any agency thereof, nor any of their employees, nor any of their contractors, subcontractors, or their employees, make any warranty, express or implied, or assume any legal liability or responsibility for the accuracy, completeness, or usefulness of any information, apparatus, product, or process disclosed, or represent that its use would not infringe privately owned rights. Reference herein to any specific commercial product, process, or service by trade name, trademark, manufacturer, or otherwise, does not necessarily constitute or imply its endorsement, recommendation, or favoring by the United States Government, any agency thereof, or any of their contractors or subcontractors. The views and opinions expressed herein do not necessarily state or reflect those of the United States Government, any agency thereof, or any of their contractors.

Printed in the United States of America. This report has been reproduced directly from the best available copy.

Available to DOE and DOE contractors from
U.S. Department of Energy
Office of Scientific and Technical Information
P.O. Box 62
Oak Ridge, TN 37831

Telephone: (865) 576-8401
Facsimile: (865) 576-5728
E-Mail: reports@adonis.osti.gov
Online ordering: http://www.osti.gov/bridge

Available to the public from
U.S. Department of Commerce
National Technical Information Service
5285 Port Royal Rd.
Springfield, VA 22161

Telephone: (800) 553-6847
Facsimile: (703) 605-6900
E-Mail: orders@ntis.fedworld.gov
Online order: http://www.ntis.gov/help/ordermethods.asp?loc=7-4-0#online

SAND2014-2858
Unlimited Release
Printed April 2014
Supersedes SAND2012-5961 dated July 2012

A Simple Model of Gas Flow in a Porous Powder Compact

Andrew D. Shugard, Gas Transfer Systems (8254)
David B. Robinson, Energy Nanomaterials (8651)
Sandia National Laboratories
P.O. Box 969
Livermore, California 94551-9291

Abstract

This report describes a simple model for ideal gas flow from a vessel through a bed of porous material into another vessel. It assumes constant temperature and uniform porosity. Transport is treated as a combination of viscous and molecular flow, with no inertial contribution (low Reynolds number). This model can be used to fit data to obtain permeability values, determine flow rates, understand the relative contributions of viscous and molecular flow, and verify volume calibrations. It draws upon the Dusty Gas Model and other detailed studies of gas flow through porous media.

ACKNOWLEDGMENTS

The authors would like to thank Hans Aichlmayr for his assistance. Hans extensively reviewed the available literature on flow in porous media and identified the Dusty Gas Model as the most relevant description of gas flow. The model description and mathematical treatment presented in this paper draw heavily from an unpublished memo written by Hans.

CONTENTS

FIGURES

NOMENCLATURE

Roman Symbols

A_c	bed cross-sectional area [cm^2]
B	effective permeability of a porous medium [cm^2]
B_{pore}	permeability of a single capillary pore [cm^2]
c	gas phase molar concentration $\left[\frac{mol}{cm^3}\right]$
d	molecular diameter [cm]
D	gas-phase binary diffusion coefficient [cm^2/s]
D^e	effective gas-phase binary diffusion coefficient [cm^2/s]
D^K	effective Knudsen diffusion coefficient [cm^2/s]
D^K_{pore}	D^K for a single capillary pore
K_0	molecular flow coefficient [cm]
L_c	axial length of the compact [cm]
L_{eff}	effective length of crooked capillary [cm]
M	gas molecular mass [g/mol]
$\dot{n}$	molar flow rate [mmol/s]
k	pressure decay constant during blowdown [s^{-1}]
P	total gas pressure [MPa]
P_0	upstream pressure at $t = 0$ [MPa]
P_1	compact upstream face pressure [MPa]
P_2	compact downstream face pressure [MPa]
P_{AVG}	average compact face pressure [MPa]
ΔP_{BED}	pressure loss across the compact [MPa]
P_{eq}	System pressure at $t = \infty$ during blowdown
P_r	pressure in receiver vessel [MPa]
P_s	pressure in source vessel [MPa]
q	tortuosity factor [dimensionless]
R	universal gas constant $\left[8.314\frac{J}{mol\ K}\right]$
r	capillary pore radius [cm]
r_h	pore hydrodynamic radius [cm]
r_{eq}	average equivalent capillary radius [cm]
S_v	surface area per unit compact volume [1/cm]
T	temperature [K]
t	time [s]
t_{ss}	time to reach steady state [s]
V_r	receiver vessel volume [cm^3]
V_s	source vessel volume [cm^3]
v	mean speed of gas molecules [cm/s]

x	mole fraction of component of gas mixture [dimensionless]
z	axial coordinate [cm]

Greek Symbols

ε	porous media void fraction (porosity) [dimensionless]
λ	mean free path of gas molecule [cm]
μ	gas viscosity [MPa s]
$\overline{\mu}$	viscosity of gas mixture [MPa s]

Vectors

$\mathbf{N}$	total superficial molar flow rate $\left[\frac{\text{mol}}{\text{cm}^2\ \text{s}}\right]$
$\mathbf{N}_\text{m}$	free molecular flow component $\left[\frac{\text{mol}}{\text{cm}^2\ \text{s}}\right]$
$\mathbf{N}_\text{v}$	viscous flow component $\left[\frac{\text{mol}}{\text{cm}^2\ \text{s}}\right]$

1. DERIVATION OF FLOW MODEL

1.1. Introduction

This paper considers non-reacting gas flow in a powder compact (or similar porous medium) at constant temperature. The goal of this report is to present a simple mathematical model for the flow properties as a function of the geometry of the compact and of the properties of the nonreacting gas. Fitting to experimental data allows empirical determination of the viscous flow (permeability) and molecular flow (Knudsen diffusion) coefficients, and evaluation of whether the model's assumptions apply. The parameters can be used to make inferences about the structure of the pores.[1,2]

The use of parallel or superimposed viscous and molecular flows follows from the Dusty Gas Model.[3] This approach can accurately describe gas transport over a wide range of conditions.[12] The model is controversial in some aspects, but not at the level of detail considered here.[4,5] With gas near room temperature and pressure flowing through μm-scale particles, the Knudsen number (ratio of mean free path to pore diameter) is ≈ 0.01 and therefore proper treatment of free molecular flow is needed for suitable accuracy.

Flow measurements are conveniently performed in two distinct experiments. The first measures pressure loss across the compact at a constant flow rate. The second uses pressure depletion from a known volume. We formulate versions of the model for each case.

1.2. Mass and Momentum Conservation

The Dusty Gas Model, developed during the 1960s, is described in a series of papers.[6,7,8,9,10] Mason and Malinauskas's monograph gives a thorough description of the model.[3] Jackson also reviews the model and demonstrates its application to porous catalysts.[11] The model combines viscous bulk flow, free-molecular flow, and molecular diffusion. It has been shown to accurately predict species transport for regimes ranging from Knudsen streaming to viscous flow.[12]

The species flux relations incorporate momentum conservation and transport. The bulk fluid velocity is related to the total pressure gradient by approximating the porous medium as a network of capillary tubes.[7] This treatment leads to the use of Darcy's law. The inertial terms of the Navier-Stokes equations are neglected, and the Dusty Gas Model is therefore limited to small Reynolds and Mach numbers. While limiting, this assumption is key to the development of the model because it allows the viscous and free molecular fluxes to be combined.[3]

1.2.1. Molar conservation

For a pure, non-reacting gas in a porous medium with a temporally and spatially invariant void fraction (porosity) ε, concentration c (mmol gas/cm^3 pore volume) and the total molar flux $\mathbf{N}$ (mmol/s-cm^2 bed cross-sectional area), the overall species balance is

$$\varepsilon \frac{\partial c}{\partial t} + \nabla \cdot \mathbf{N} = 0 \tag{1}$$

for a control volume much larger than the medium's average pore size.[13] The porosity factor converts between variables describing the pore space (such as concentration) and those describing the entire compact (such as molar flux).

Porosity variation is a foreseeable complication. Its magnitude can depend on the packing technique, the results of which can be affected by particle shape, and particle-particle and particle-wall friction. Mason and Malinauskas provide a detailed discussion of the assumption of uniform porosity and its limitations.[3] Contrast variations observed in radiography can diagnose nonuniformity, and some flow tests discussed below may help identify it.

1.2.2. Viscous Flow

Gas flow through a porous medium is well described by Darcy's law, provided the flow is laminar within the pores, and the pore diameter is large relative to the molecular mean free path.[3]

$$\mathbf{N}_\mathbf{v} = -\frac{B}{\mu} c \nabla P. \tag{2}$$

where $\mathbf{N}_\mathbf{v}$ is the molar flux due to viscous flow (mmol/cm^2-s), P is the pressure (MPa), μ is the viscosity (MPa-s), and B is the permeability (cm^2). If there were only a single, straight pore of circular cross section, Darcy's law is essentially a restatement of Poiseuille's law for laminar incompressible flow through a pipe, which relates a pressure drop to a volumetric flow rate. Rearranging Darcy's law gives

$$\nabla P = -\frac{\mu}{B A_c}\left(\frac{A_c \mathbf{N}_\mathbf{v}}{c}\right) \tag{3}$$

where A_c (cm^2) is the cross-sectional area of the pipe, the factor in parentheses is a volumetric flow rate, and the denominator of the prefactor has units of cm^4. Analogy with Poiseuille's law gives $B_{pore} = A_c/8\pi$.

Because a cross section of the compact contains an array of pores through an occluded area, we must include the porosity factor in B. Also, the irregular nature of the solid phase creates a tortuous path that the fluid must follow as it traverses the compact, so the average fluid path length L_{eff} exceeds the superficial compact length L_c. The porous medium can thus be modeled as a bundle of crooked capillary tubes. In this case, the effective permeability is related to the permeability of a single pore by,

$$B = \frac{\varepsilon}{q} B_{pore}, \tag{4}$$

where the tortuosity factor $q = \left(L_{eff}/L_c\right)^2$. (The tortuosity captures one factor of the length ratio because the flux is reduced when averaged over the many pore orientations, and another from the additional path length in the pressure gradient.) In a real porous medium, pores are irregular, interconnected, and typically have radii on the order of the length of the passage. Mason and Malinauskas describe details of the capillary model and its limitations.[3]

While the details of pore geometry are difficult to quantify, it is often straightforward to measure the internal surface area of the pores per gram of powder, or per cm^3 of the compact S_v. For an array of uniform, straight cylindrical pores of radius r, the surface area per unit pore volume is $S_v/\varepsilon = 2\pi r L_c/A_c L_c = 2/r$. This can be rearranged to define an equivalent capillary radius r_{eq} for the porous medium.

$$r_{eq} = \frac{2\varepsilon}{S_v} \tag{5}$$

By the Poiseuille flow analogy, $B_{pore} = \frac{r_{eq}^2}{8}$. Equation (4) then becomes

$$B = \frac{\varepsilon}{q}\frac{r_{eq}^2}{8}. \tag{6}$$

Using the definition of equivalent capillary radius, r_{eq} can be eliminated in favor of ε and S_v, giving

$$B = \frac{1}{2}\frac{\varepsilon}{q}\frac{\varepsilon^2}{S_v^2}. \tag{7}$$

From his experiments on sintered frits, Meyer[1] found (but stated differently) that q was correlated with ε by

$$q = \frac{1.25}{\varepsilon^{1.1}} \tag{8}$$

Meyer estimates the accuracy of q to be $\pm 30\%$ of the predicted value. Perfect agreement is not anticipated because morphological differences between sintered frits and unconsolidated sample powders may change the relationship between q and ε. Substitution of Equation (8) into Equation (7) gives Meyer's correlation for effective permeability,

$$B = 0.4\frac{\varepsilon^{4.1}}{S_v^2} \tag{9}$$

The permeability correlation was developed by studying flow in sintered stainless steel frits with $0.18 < \varepsilon < 0.67$ and $2\times10^{2} < S_v < 1.4\times10^{3}$ cm^{-1}. However, it is probably justifiable to extrapolate this correlation to values outside these ranges to a modest degree.

The system is assumed isothermal, and the gas is assumed ideal, so $P = cRT$, where R is the ideal gas constant (J/mmol K), and T is the temperature (K). This allows elimination of c in favor of P, which is more easily measured.

$$\mathbf{N}_{\mathbf{v}} = -\frac{BP}{\mu RT}\nabla P \tag{10}$$

These two assumptions are justified for non-reacting gas flow at near-ambient temperature and low to moderate pressure. The compressibility, Z, is a coefficient in the real gas law, $P = ZcRT$, describing deviation from ideality. As examples, at 4 MPa and 295 K, the compressibility of helium is 1.02, indicating a 2% deviation from ideal gas behavior.[14] At 1 MPa and 295 K, the compressibility is approximately 1.005. The isothermal assumption is appropriate when the gas is non-reacting and the flow is near steady-state. In many experiments, localized heating or cooling from rapid compression or expansion of the gas is not significant. In those cases, the temperature within the compact can be assumed to be both invariant in time and spatially uniform without introducing a significant error.

1.2.3. Free molecular flow

An additional contribution to the flux is free molecular flow. This flux is controlled by collisions between gas molecules and pore walls. Because the individual molecules follow paths that can be described as random walks, their net flux is modeled as diffusion along a concentration gradient (using Fick's law).

$$\mathbf{N}_{\mathbf{m}} = -D^{K}\nabla c \tag{11}$$

where $\mathbf{N_m}$ is the free-molecular contribution to the flux and D^K is the effective Knudsen diffusion coefficient. Application of the ideal gas law gives

$$\mathbf{N}_{\mathbf{m}} = -\frac{D^{K}}{RT}\nabla P \tag{12}$$

Free-molecular transport dominates when gas molecule-wall collisions occur much more frequently than molecule-molecule collisions. In other words, it dominates when the mean free path λ greatly exceeds the pore diameter. [15]

$$\lambda = \frac{2\mu}{Mcv} = \frac{\pi\mu}{4RTc}\sqrt{\frac{8RT}{\pi M}} >> 2r \tag{13}$$

where v is the mean speed of the gas molecules (cm/s) and is equal to the square root factor in Equation (13).

For a circular capillary having a constant radius and $L >> r$ with perfectly diffuse scattering of the gas molecules by the tube walls, D^K_{pore} is given by

$$D^K_{pore} = \frac{2}{3} r v = \frac{2}{3} r \left(\frac{8RT}{\pi M} \right)^{1/2} \tag{14}$$

This is the product of a path length comparable to the pore dimensions, and the thermal speed of the gas molecules. Thus the Knudsen diffusion coefficent is pressure-independent.

The effective D^K, which applies to the entire compact, is related to the pore Knudsen diffusion coefficient using a similar model of a bundle of crooked capillaries.

$$D^K = \frac{\varepsilon}{q} D^K_{pore}. \tag{15}$$

Substitution of Equation (14) into Equation (15) gives

$$D^K = \frac{2}{3} \frac{\varepsilon}{q} r_{eq} \left(\frac{8RT}{\pi M} \right)^{1/2} \tag{16}$$

where we are using the radius derived from the surface area measurement. Mason and Malinauskas[3] provide a different parameterization of the Knudsen diffusion coefficient D^K, as

$$D^K = \frac{4}{3} K_0 \left(\frac{8RT}{\pi M} \right)^{1/2}, \tag{17}$$

where K_0 is an empirical parameter. Fits to flow data are sometimes reported as K_0 instead of D^K, to keep the compact geometry parameters, K_0 or r_{eq}, separate from $\left(\frac{8RT}{\pi M} \right)^{1/2}$.

1.2.4 Multi-Component Transport

The additional complexity associated with multi-component transport is considered by the Dusty Gas Model and briefly described here. Multi-component diffusion can be significant for gas mixtures when the pressure is high enough that molecule-molecule collisions are much more frequent than molecule-wall collisions. The molecular diffusion flux is included in the Dusty Gas Model by incorporating the Stefan-Maxwell transport equations,

$$-\nabla x_i = \sum_{\substack{j=1 \\ j\neq i}}^{n} \frac{x_j \mathbf{N}_i - x_i \mathbf{N}_j}{c D_{ij}^e} \tag{18}$$

where x_i is the mole fraction of species i, x_j is the mole fraction of species j, $\mathbf{N}_i$ is the superficial flux of species i, $\mathbf{N}_j$ is the superficial flux of species j, and D_{ij}^e is the effective binary molecular diffusion coefficient for species pair ij. The effective molecular diffusion coefficient is simply the normal binary molecular diffusion coefficient for the species pair, D_{ij}, suitably corrected for the porosity and tortuosity of the compact. If one assumes a crooked capillary model, then

$$D_{ij}^e = \frac{\varepsilon}{q} D_{ij} . \tag{19}$$

Including multi-component diffusion significantly increases the model's mathematical complexity. To find the flux of species i in a mixture of n species, when both free-molecular and viscous transport are significant, one must simultaneously solve a system of n flux equations. The flux equations, which incorporate viscous, free-molecular, and diffusive transport, are,

$$\frac{\mathbf{N}_i}{D_i^K} + \sum_{\substack{j=1 \\ j\neq i}}^{n} \frac{x_j \mathbf{N}_i - x_i \mathbf{N}_j}{D_{ij}^e} = -\frac{P}{RT}\nabla x_i - \frac{x_i}{RT}\left(1 + \frac{BP}{\bar{\mu} D_i^K}\right)\nabla P . \tag{20}$$

where $\bar{\mu}$ is the average viscosity of the gas mixture. The average viscosity of a gas mixture containing n species may be estimated by Wilkie's semi-empirical formula[16],

$$\bar{\mu} = \sum_{i=1}^{n} \frac{x_i \mu_i}{\sum_{j=1}^{n} x_j \Phi_{ij}} \tag{21}$$

where

$$\Phi_{ij} = \frac{1}{\sqrt{8}}\left(1 + \frac{M_i}{M_j}\right)^{-1/2}\left[1 + \left(\frac{\mu_i}{\mu_j}\right)^{1/2}\left(\frac{M_j}{M_i}\right)^{1/4}\right]^2 . \tag{22}$$

Here x_i and x_j are the mole fraction of species i and j, μ_i and μ_j are the viscosity of species i and j, and M_i and M_j are the corresponding molecular weights.

1.2.5 Single-Component Momentum Conservation

Incorporating multicomponent transport greatly complicates the Dusty Gas Model. Fortunately however, for our conditions, namely a pure non-reacting gas, ∇x_i and the second term on the left hand side are zero. Therefore Equation (20) can be reduced to

$$\mathbf{N} = -\frac{BP}{\mu RT}\nabla P - \frac{D^K}{RT}\nabla P\,, \tag{23}$$

as we would expect, because it is the sum of the viscous and free-molecular flux contributions given by Equations (10) and (12). We refer to this as a momentum conservation equation because the gas and the particles of the bed exert forces on each other in order to establish this relationship between pressure and molar flow rate. The molar flow rate can be expressed as a product of the gas concentration and its bulk flow velocity. When **N** and T are uniform in space and time, the pressure and velocity are inversely proportional.

1.2.6 Comparison of Viscous and Free-Molecular Flow

Equation (23) shows that in the low-pressure limit, $BP/\mu D^K << 1$, free-molecular flux dominates, and that as P increases, viscous flux increases, until it eventually becomes dominant.

Expressions derived above can be used to compare the magnitudes of the two contributions to the flux, which both depend on the pressure gradient. If the free-molecular contribution is greater, after converting pressure to concentration,

$$\frac{D^K}{RT} > \frac{Bc}{\mu}\,. \tag{24}$$

By incorporating the crooked capillary expressions, Eqs. (6) and (16), this can be rearranged to

$$\frac{32\mu}{3RTc}\sqrt{\frac{8RT}{\pi M}} >> 2r \tag{25}$$

which is similar to Equation (13). The Knudsen diffusion coefficient can also be related to the effective permeability through the equivalent capillary radius. By combining Equations (6) and (8),

$$r_{eq} = \left(\frac{8qB}{\varepsilon}\right)^{1/2} = \left(\frac{10B}{\varepsilon^{2.1}}\right)^{1/2}. \tag{26}$$

and combining Equations (16) and (8),

$$D^K = 1.69\varepsilon^{1.05}B^{1/2}\left(\frac{8RT}{\pi M}\right)^{1/2} \tag{27}$$

Again, this is limited by the assumptions of the crooked capillary model and the accuracy of the tortuosity correlation, but it provides a basic concept for the scaling of these transport parameters. As a footnote, Meyer is careful to refer to r_{eq} as the average pore radius. Others

have called r_{eq} the hydraulic radius r_h, which is incorrect. The quantities differ by a factor of 2, with $r_{eq} = 2r_h$.[17]

The Knudsen diffusion coefficient can also be compared to the viscosity. In a hard-sphere model, the viscosity takes the form

$$\mu = 0.0049 \frac{M}{d^2} \left(\frac{8RT}{\pi M} \right)^{1/2} \tag{28}$$

where d is the molecular diameter. This is modified by longer-range interactions in a real gas.[15] Because viscosity appears in the denominator, this suggests that viscous flux is reduced and free-molecular flux increased with increasing temperature, and that both terms decrease when the molecular weight is increased (assuming no change in d, as expected upon substitution by a different isotope).

2. APPROACH TO SPATIALLY UNIFORM FLUX

2.1. Introduction

The substitution of the momentum conservation equation (23) into the mass conservation equation (1) leads to a general description of the time and spatial dependence of the properties of the compact. However, it is relatively difficult to solve. Simpler, closed-form solutions can be obtained if we can justify an assumption of spatially uniform flux: $\frac{\partial \mathbf{N}}{\partial z} = 0$. To determine the validity of this assumption, we compare the time for a compact to reach steady-flow conditions with the duration of a typical experiment. If the compact's steady-state relaxation time is much shorter than the time to reach pressure equilibrium, then the steady-state assumption is justified.

As before, the system is assumed isothermal, the compact is assumed uniform, the fluid viscosity is assumed constant, and the fluid is taken to be a pure, ideal gas. The combined governing equations take the following form (using the ideal gas law to eliminate concentration):

$$\frac{\partial P}{\partial t} = \frac{B}{\varepsilon \mu}\left[\left(\frac{\partial P}{\partial z}\right)^2 + P\frac{\partial^2 P}{\partial z^2}\right] + \frac{D^K}{\varepsilon}\frac{\partial^2 P}{\partial z^2}. \tag{29}$$

Equation (29) can be solved to give the fluid's molar concentration within the compact as a function of time to determine the time needed to reach a spatially constant molar flux. Taken with the boundary conditions imposed by the geometry of the compact, the equation does not always have a simple analytic solution. We will present some special cases that make the behavior of the system quite clear.

2.2. Steady State Concentration Profile

At steady state, Equation (29) reduces to

$$0 = \frac{B}{\mu}\left[\left(\frac{dP}{dz}\right)^2 + P\frac{d^2 P}{dz^2}\right] + D^K\frac{d^2 P}{dz^2}. \tag{30}$$

and we know that flux is spatially uniform from the mass conservation equation (1). For a compact of length L_c, with boundary conditions of $P(0) = P_1$ and $P(L) = P_2$, Equation (29) can be solved exactly. The solution is

$$\frac{P(z)}{P_1} = -\frac{D^K \mu}{BP_1} + \sqrt{1 - \left(1 - \frac{P_2^2}{P_1^2}\right)\frac{z}{L_c} + 2\frac{D^K \mu}{BP_1}\left[1 - \left(1 - \frac{P_2}{P_1}\right)\frac{z}{L_c}\right] + \left(\frac{D^K \mu}{BP_1}\right)^2} \tag{31}$$

When P_1 is high, and flow is primarily viscous, this has the limiting case

$$\frac{P(z)}{P_1} = \sqrt{1-\left(1-\frac{P_2^2}{P_1^2}\right)\frac{z}{L_c}} \tag{32}$$

and when P_1 is low, and transport is free molecular, the pressure drop is linear:

$$\frac{P(z)}{P_1} = 1-\left(1-\frac{P_2}{P_1}\right)\frac{z}{L_c} \tag{33}$$

Because the molar flow rate is constant, as noted in 1.2.5, the gas velocity is inversely proportional to pressure.

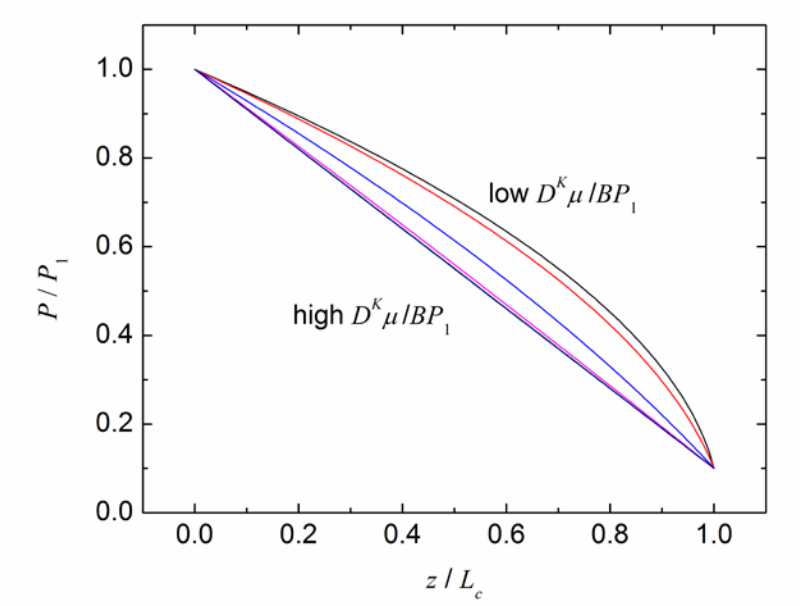

Figure 1. Steady state pressure profiles for several values of $\frac{D^K \mu}{BP_1}$. Its value is 1 for the middle curve, and varies by factors of 10 on either side. The pressure drop is tenfold across the compact.

Figure 1 shows that the concentration profile is linear when free-molecular transport dominates. When viscous flow dominates, the gas moves more slowly at higher concentration, but accelerates as the concentration decreases. With other conditions constant, the molar flow rate in viscous flow is higher than for free molecular transport because the pressure is higher. Figure 1 is normalized to highlight the shapes of the curves, and not their relative scale, for different flow regimes. The asymmetry of the profile in the viscous regime can be a way to measure nonuniform porosity: if two flow experiments are performed in opposite directions, one could expect different results.

2.3. Transient Numerical Solution

The solution to Equation (29), in the case where P_1 is small and the viscous term is negligible, is given by

$$P(z) = P_2 + (P_1 - P_2)\left[\frac{\operatorname{erfc}\left(\frac{z}{\sqrt{4D^K t/\varepsilon}}\right) - \operatorname{erfc}\left(\frac{2L_c - z}{\sqrt{4D^K t/\varepsilon}}\right)}{1 + \operatorname{erfc}\left(\frac{2L_c}{\sqrt{4D^K t/\varepsilon}}\right)}\right] \tag{34}$$

Most notable about this solution is that it is close to steady state when the argument in the error function in the denominator is less than 1, or at times greater than $\varepsilon L_c^2/D^K$. From this and further inspection of Equation (29), one might speculate that the timescale for approach to steady state in the viscous case could be estimated as $\varepsilon\mu L_c^2/BP_1$.

Equation (29) was solved using a finite difference method implemented in GNU Octave. The method used central differencing for the space derivatives and backward differencing for the time derivative. This is commonly referred to as an explicit, central difference scheme.

Solutions were computed for conditions representative of blowdown experiments. The pressures at the upstream and downstream faces of the compact are P_1 and $0.1P_1$ respectively, with varying P_1 values. The initial pressure within the compact was determined from Equation (34) evaluated at a small value of *t*. The grid size is 101 points and time step is 10^{-6} seconds. L_c is 10 mm, D^K is 100 mm^2/s, B/μ is 10^4 mm^2/MPa s, and ε is 0.75. Under these conditions, for $P_1 << D^K\mu/B$, we would expect the time to steady state to be 0.75 s, and once those pressures become comparable, that time should decrease with increasing pressure.

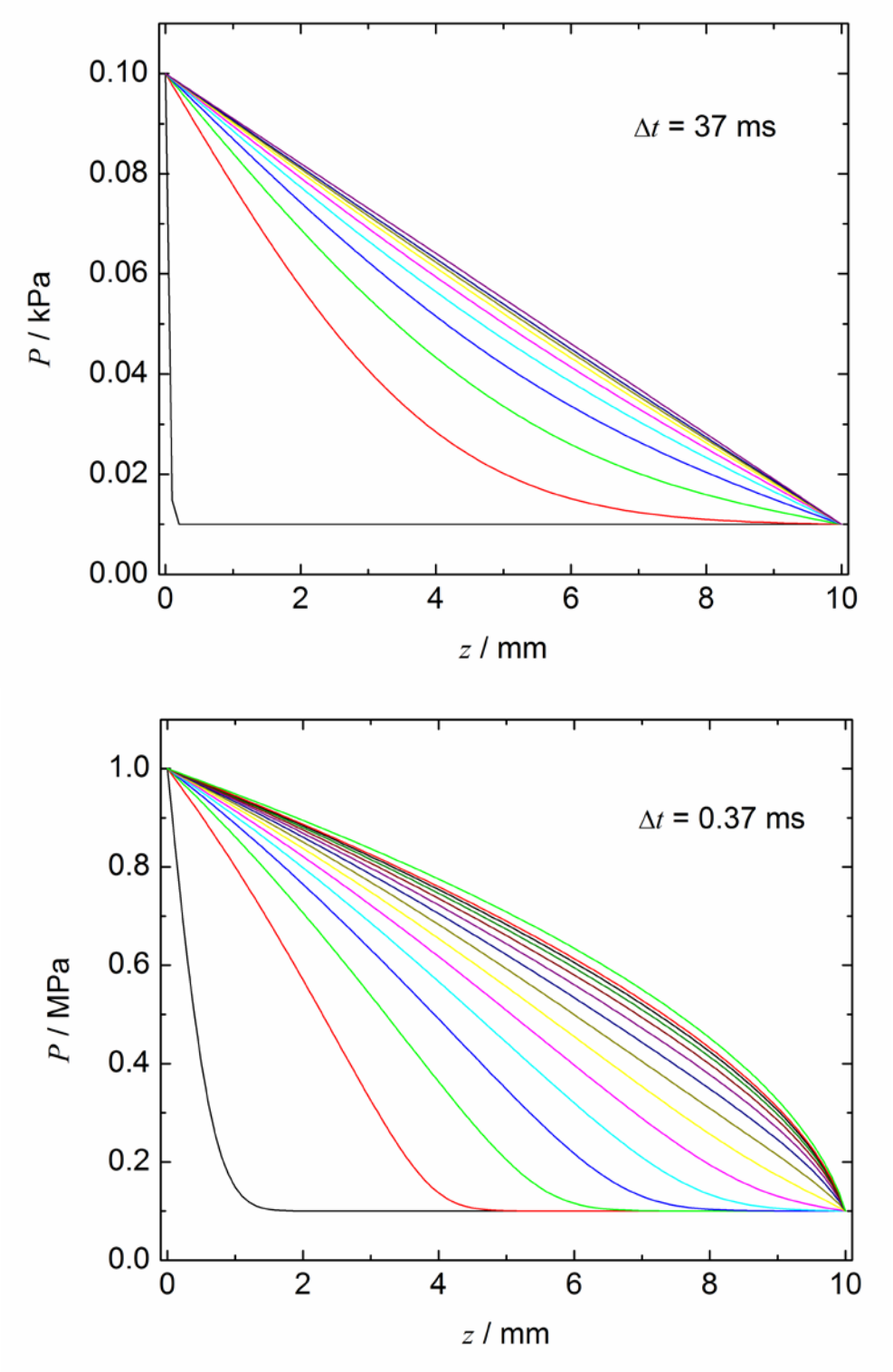

Figure 2. Plot of transient solutions for time points separated by the interval shown. The upper plot is for a low-pressure case where free-molecular flow dominates, whereas the lower plot is for a high-pressure case where viscous flow dominates.

Figure 2 shows simulation results at a low pressure, where free-molecular flow dominates, and at high pressure, where viscous flow dominates. These and other results show that the estimated times to steady state are reliable, and more generally, the time t_{ss} can be estimated by

$$t_{ss} = \varepsilon L_c^2 / \left(D^K + B P_1 / \mu \right) \tag{35}$$

As will be shown, vessel volumes and the compact diameter can be chosen to ensure that the experiment lasts significantly longer than this.

3. APPLICATION TO EXPERIMENTAL CASES

3.1. Steady Flow

Assuming a uniform compact reduces the analysis to one space dimension, and assuming steady flow (constant flow rate) eliminates the time dimension from the mass conservation equation (1). This gives

$$\frac{d\mathbf{N}}{dz} = 0 \tag{36}$$

and from the transport equation (23)

$$\mathbf{N} = -\frac{BP}{\mu RT}\frac{dP}{dz} - \frac{D^K}{RT}\frac{dP}{dz} \tag{37}$$

For steady flow tests, Equation (37) can be evaluated for a compact of length L_c and superficial area A_c with face pressures P_1 and P_2. Equation (37) can be separated and integrated over the length of the compact, giving

$$\frac{\dot{n}}{A_c} = \frac{B}{2\mu RTL_c}\left(P_1^2 - P_2^2\right) + \frac{D^K}{RTL_c}\left(P_1 - P_2\right) \tag{38}$$

where $\dot{n}$ is the molar flow rate (mmol/s).

Equation (38) can be rearranged into a form more suitable for analysis if one notes that $\left(P_1^2 - P_2^2\right) = \left(P_1 + P_2\right)\left(P_1 - P_2\right)$ and defines $P_{AVG} = \frac{1}{2}\left(P_1 + P_2\right)$ and $\Delta P_{BED} = P_1 - P_2$, giving

$$\frac{\dot{n}RTL_c}{A_c \Delta P_{BED}} = \frac{B}{\mu} P_{AVG} + D^K \tag{39}$$

This is a very illustrative form for the solution. The first and second terms on the right hand side represent the flux contributions from free-molecular and viscous flow respectively.
Experimentally, steady flow can be achieved or approximated by use of a regulated gas cylinder, which applies a constant pressure to one side of a compact, and by venting the other end of the compact to the atmosphere.

3.2. Blowdown

In a blowdown test, vessels of finite volume are connected to each end of the compact. One vessel is isolated by a valve, and each vessel is loaded to a different initial pressure. The valve is opened, and the pressures are allowed to equilibrate. The analysis of the previous section still applies, but the pressures and flow rate are now time-dependent.

Maintaining constant temperature can be difficult due to adiabatic expansion from one vessel and compression in the other. Monitoring of temperature within each vessel is important. If the timescale of the experiment is long enough, the surface-to-volume ratio of the vessels and tubing are high enough, or other measures are taken to increase contact of the gas with surfaces of relatively uniform temperature, the gas temperature variations can be kept small. In the isothermal case, the analysis is greatly simplified, and Equations (1) and (37) can be solved in closed form. For the sake of simplicity, this assumption is utilized, and a possible loss of model fidelity is accepted.

To analyze the blowdown test, a material balance is performed on the vessel, and an ideal gas is assumed. We call the vessel with higher pressure the "source" and the lower pressure the "receiver". This gives

$$\dot{n} = -\frac{V_s}{RT}\frac{dP_s}{dt}. \tag{40}$$

where V_s is the constant source volume and P_s the time-dependent source pressure. The mass flow rates at the inlet and outlet of the compact are assumed to be equal (no gas is absorbed or released in the compact), which implies that $\frac{d\mathbf{N}}{dz} = 0$. Consequently, the molar flux, $\dot{n}/A_c$, is given by Equation (38), replacing P_1 and P_2 with P_s and P_r, the receiver pressure. These assumptions allow Equations (38) and (40) to be combined, giving

$$\frac{dP_s}{dt} = -\frac{A_c}{L_c V_s}\left[\frac{B}{2\mu}\left(P_s + P_r\right) + D^K\right]\left(P_s - P_r\right) \tag{41}$$

A mole balance on the whole system before and after the experiment gives

$$P_s V_s + P_r V_r = P_{eq}\left(V_s + V_r\right) \tag{42}$$

where P_{eq} is the equilibrium pressure, which can be computed from the initial vessel pressures using this equation. The time dependence of the receiver pressure can be obtained from this equation once the time-dependent source pressure is solved. The compact is initially at equilibrium with one of the two vessels, and its void volume is lumped with the volume of that vessel. We take that vessel to be the receiver, and eliminate the receiver pressure to obtain

$$\frac{dP_s}{dt} = -\frac{A_c}{L_c}\left(\frac{1}{V_s}+\frac{1}{V_r}\right)\left[\frac{B}{2\mu}\left[P_s\left(1-\frac{V_s}{V_r}\right)+P_{eq}\left(1+\frac{V_s}{V_r}\right)\right]+D^K\right]\left(P_s-P_{eq}\right) \tag{43}$$

It can be shown that a pressure function of the form

$$P(t)=\frac{a+be^{-kt}}{f+ge^{-kt}} \tag{44}$$

solves

$$\frac{dP}{dt}=\frac{-k}{bf+ag}\left[gP+b\right]\left[fP-a\right] \tag{45}$$

which matches the form of Equation (43). The boundary conditions are $P(t=0)=P_0$, the initial value of P_s, and $P(t=\infty)=P_{eq}$. Substitution allows elimination of *a* and *f*, so

$$P_s(t)=\frac{P_{eq}\left(b+gP_0\right)+\left(P_0-P_{eq}\right)be^{-kt}}{\left(b+gP_0\right)-\left(P_0-P_{eq}\right)ge^{-kt}} \tag{46}$$

which satisfies the boundary conditions, and solves

$$\frac{dP_s}{dt}=\frac{-k}{b+gP_{eq}}\left[gP+b\right]\left[P-P_{eq}\right] \tag{47}$$

By matching coefficients, we then identify

$$k=\frac{A_c}{L_c}\left(\frac{1}{V_s}+\frac{1}{V_r}\right)\left[\frac{BP_{eq}}{\mu}+D^K\right] \tag{48}$$

$$b=\left[\frac{BP_{eq}}{2\mu}\left(1+\frac{V_s}{V_r}\right)+D^K\right] \tag{49}$$

$$g=\frac{B}{2\mu}\left(1-\frac{V_s}{V_r}\right) \tag{50}$$

This closed form can easily be used in a spreadsheet or other data analysis software. P_r can be computed similarly, deriving the appropriate initial condition from Equation (42) and swapping V_s and V_r in Equations (49) and (50). Several especially simple cases can be identified. If the vessel volumes are equal,

$$P_s(t) = P_{eq} + (P_0 - P_{eq})e^{-kt} \tag{51}$$

$$P_r(t) = P_{eq} - (P_0 - P_{eq})e^{-kt} \tag{52}$$

$$k = \frac{2A_c}{L_c V_s}\left[\frac{BP_{eq}}{\mu} + D^K\right] \tag{53}$$

noting also that P_{eq} is simply the average of the upstream and downstream pressures in this case. If $V_r = \infty$, or the compact is vented to the atmosphere or into a vacuum pump at pressure P_2, the result is

$$P_s(t) = \frac{(P_0 - P_2)(BP_2 + 2D^K\mu)e^{-kt} + P_2(B(P_0 + P_2) + 2D^K\mu)}{B(P_2 - P_0)e^{-kt} + (B(P_0 + P_2) + 2D^K\mu)}, \tag{54}$$

where

$$k = \frac{A_c(BP_2 + D^K\mu)}{\mu L_c V_s}. \tag{55}$$

Some other simplified cases can be obtained if only one transport regime (viscous or free-molecular flow) prevails throughout the experiment. For free-molecular transport only,

$$P_s(t) = P_{eq} + (P_0 - P_{eq})e^{-kt} \tag{56}$$

$$k = \frac{A_c D^K}{L_c}\left(\frac{1}{V_s} + \frac{1}{V_r}\right) \tag{57}$$

For viscous flow only:

$$P_s(t) = P_{eq}\frac{1 + \beta(V_r + V_s)e^{-kt}}{1 - \beta(V_r - V_s)e^{-kt}} \tag{58}$$

$$k = \frac{A_c BP_{eq}}{\mu L_c}\left(\frac{1}{V_s} + \frac{1}{V_r}\right) \tag{59}$$

$$\beta = \frac{(P_0 - P_{eq})}{P_0(V_r - V_s) + P_{eq}(V_r + V_s)} \tag{60}$$

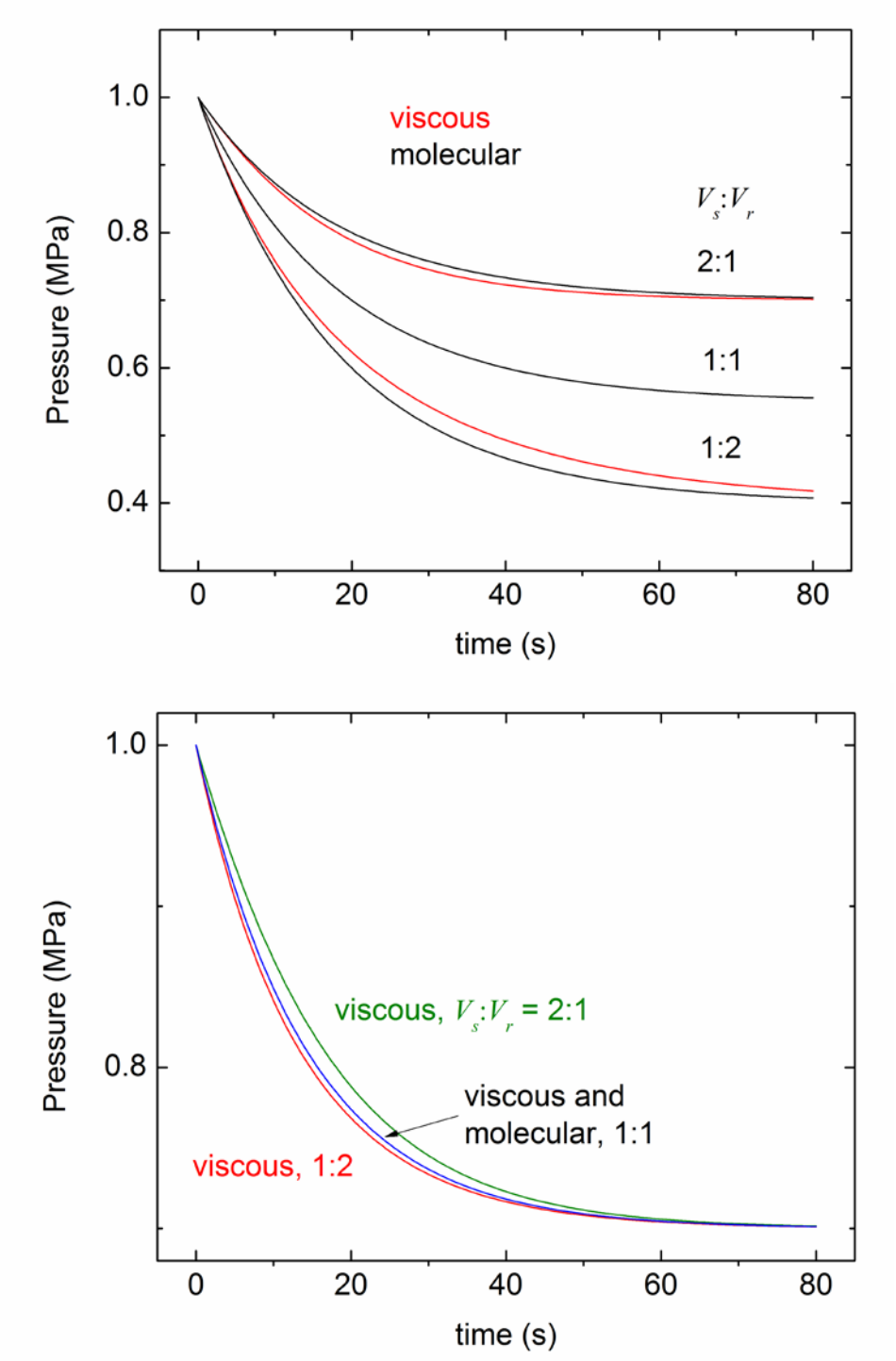

Figure 3. Response in each flow regime to varying conditions. Curve label indicates V_s to V_r ratio. Top plot uses constant pressure ratio of 10, while bottom plot adjusts P_r to maintain constant P_{eq}. D^K was set to match viscous case when volumes are equal.

Figure 3 compares the predicted pressure traces for the cases of purely viscous or purely free molecular flow under varying conditions. All molecular flow curves are simple exponentials, as

is the viscous flow curve for equal volumes. However, when the volumes are different, more complex behavior is exhibited by the viscous case. Under some conditions it is faster than the exponential, and sometimes slower, depending on the initial pressures and volumes. The equal-volume case greatly simplifies experimental interpretation, and fitting to experimental data. The shape changes can be subtle, so determining the flow regime from the curve shape can be difficult. However, even when the volumes are equal, and the curve shape does not depend on the flow regime, that regime can still be identified by performing the experiment at different initial pressures, or with gases of differing viscosity (though less easily through isotopic substitution, as noted above, because D^K and μ scale similarly with molecular weight).

As mentioned earlier, assuming the compact is in steady state during the transient blowdown is not strictly correct. The tubing between the valve and compact will rapidly equilibrate with the source vessel, and gas in the compact will pressurize until a relatively smooth pressure drop is obtained. Because the volumes involved are much smaller than the vessel volumes and the resistance to flow is lower than that of the whole compact, this response is typically much faster, and the effect is easily corrected for experimentally by adjusting P_0 to the value just after this transient, and V_s to include the tubing and about half of the compact void volume (reducing V_r accordingly). The analysis of the spatial concentration profile in the previous chapter can help identify or justify a suitable correction.

3.3. Flow rate analysis

Alternatively, the time-dependent flow rate in a blowdown experiment can be found from the known time-dependent pressures using Equation (41). One advantage of this method is that it allows one to correct for pressure drops from the frits at either end of the compact, the flow parameters of which can be measured in flow tests on an empty column. A disadvantage is that it requires numerical computation of the time derivative of pressure. The pressure derivative can computed through a difference between two sequential pressure measurements divided by the time interval between them, but this amplifies high-frequency noise in the data. The noise can be mitigated by averaging the differences (or equivalently by using pressure measurements separated by larger time intervals), or experimentally by reducing the bandwidth of the pressure transducer signal. These approaches are less effective (or degrade the data) near the beginning of the dataset, which may contain valuable information. However, there can be value in comparing results from a flow rate analysis to direct fits of the time-dependent pressure data to an equation such as (46). For example, this can show whether the improved accuracy from a frit correction outweighs the lost precision caused by numerical differentiation-amplified noise when determining flow parameters.

4. SUMMARY

This report presents the basic concepts of gas transport in porous media, and applies them in simple forms that facilitate rapid analysis of experimental data, as well as critical understanding of an experiment. It identifies several closed-form solutions of the governing equations that are easily implemented in spreadsheet or other data analysis software. This approach can be a valuable complement to more complex models, such as finite element analyses of 3D flow distributions that account for inlet geometry, pressure drops in tubing, uptake and release by the solid phase, temperature variations, nonuniform porosity, gas nonideality, turbulent or compressible flow, multi-component transport, and other effects. The insights presented here can also aid experimental design to minimize the importance of many of these complications. We hope that this report will serve as a succinct introduction to the technical field for new researchers and engineers, and a useful reference for veteran practitioners.

5. REFERENCES

[1]Meyer, B. A. and Smith, D. W. Flow Through Porous Media: Comparison of Consolidated and Unconsolidated Materials. Sandia Technical Report, SAND83-8788, Sandia National Laboratories, 1983.

[2] Meyer, B. A. and Smith, D. W. Flow Through Porous Media: Comparison of Consolidated and Unconsolidated Materials. *Industrial and Eng. Chem. Fundamentals*, 24:360-368, 1985.

[3] Mason, E. A. and Malinauskas, A. P. *Gas Transport in Porous Media: The Dusty-Gas Model*. Elsevier, Amsterdam, 1983.

[4] Young, J. B. and Todd, B. Modeling of multi-component gas flows in capillaries and porous solids, *Int. J. Heat Mass Transfer*, 48 (2005) 5338-5353

[5] Kerkhof, P. J. A. M. New Light on Some Old Problems: Revisiting the Stefan Tube, Graham's Law, and the Bosanquet Equation. *Industrial and Eng.Chem. Research*, 36(3):915-922, 1997.

[6] Evans III, R. B. and Watson, G. M. and Mason, E. A. Gaseous Diffusion in Porous Media at Uniform Pressure. *J. Chem. Phys.*, 35(6):2076-2083, 1961.

[7] Evans III, R. B. and Watson, G. M. and Mason, E. A. Gaseous Diffusion in Porous Media. II. Effect of Pressure Gradients. *J. Chem. Phys.*, 36(7):1894-1902, 1962.

[8] Mason, E. A. and Evans III, R. B. and Watson, G. M. Gaseous Diffusion in Porous Media. III. Thermal Transpiration. *J. Chem. Phys.*, 38(8):1808-1826, 1963.

[9] Mason, E. A. and Malinauskas, A. P. Gaseous Diffusion in Porous Media. IV. Thermal Diffusion. *J. Chem. Phys.*, 41(12):3815-3819, 1964.

[10] Mason, E. A. and Malinauskas, A. P. and Evans III, R. B. Flow and Diffusion in Porous Media. *J. Chem. Phys.*, 46(8):3199-3216, 1967.

[11] Jackson, R. *Transport in Porous Catalysts*. Elsevier, Amsterdam, 1977.

[12] Webb, Stephen W. Gas-Phase Diffusion in Porous Media---Evaluation of an Advective-Dispersive Formulation and the Dusty-Gas Model for Binary Mixtures. *J. Porous Media*, 1(2):187-199, 1998.

[13] Bird, R. Byron and Stewart, Warren E. and Lightfoot, Edwin N. *Transport Phenomena*. John Wiley and Sons, New York, 1960.

[14] McLinden, M. O. and Lemmon, E. W. and Klein, S. A. and Peskin, A. P. NIST Standard Reference Database 12 v. 5.0. National Institute of Standards and Technology, 2005.

[15] Kee, R. J., Coltrin, M. E., and Glarborg, P. *Chemically Reacting Flow: Theory and Practice*. Wiley, 2005.

[16] Bird, R.B., *Transport Phenomena*. Wiley, New York, 1960.

[17] White, Frank M. *Fluid Mechanics*. McGraw Hill, New York, Fifth edition, 2003.

DISTRIBUTION

1	MS9161	George M. Buffleben	8651
1	MS9291	David B. Robinson	8651
1	MS9661	Andrew D. Shugard	8254
1	MS0899	Technical Library	9536 (electronic copy)


Sandia National Laboratories